Detecting Abnormal Pattern of Epileptic Seizures via Temporal Synchronization of EEG Signals

Miaolin Fan and Chun-An Chou

Abstract*—*Objective: **Synchronization phenomena of epileptic electroencephalography (EEG) have long been studied. In this study, we aim at investigating the spatial-temporal synchronization pattern in epileptic human brains using the spectral graph theoretic features extracted from scalp EEG and developing an efficient multivariate approach for detecting seizure onsets in real time.** ***Methods:*** **A complex network model is used for representing the recurrence pattern of EEG signals, based on which the temporal synchronization patterns are quantified using the spectral graph theoretic features. Furthermore, a statistical control chart is applied to the extracted features overtime for monitoring the transits from normal to epileptic states in multivariate EEG systems.** ***Results:*** **Our method is tested on 23 patients from CHB-MIT Scalp EEG database. The results show that the graph theoretic feature yields a high sensitivity (~98%) and low latency (~6 s) on average, and seizure onsets in 18 patients are 100% detected.** ***Conclusion:*** **Our approach validates the increased temporal synchronization in epileptic EEG and achieves a comparable detection performance to previous studies.** ***Significance:*** **We characterize the temporal synchronization patterns of epileptic EEG using spectral network metrics. In addition, we found significant changes in temporal synchronization in epileptic EEG, which enable a patient-specific approach for real-time seizure detection for personalized diagnosis and treatment.**

***Index Terms*—Complex network, data fusion, epileptic seizure, nonlinear dynamics, scalp epileptic electroencephalography (EEG), spectral graph theory.**

I. Introduction

EPILEPSY is a common neurological disorder that is characterized by a sudden surge of abnormal electrical activities (epileptic seizure onsets) in the partial or whole brain regions [1]. The seizure onset events are highly unpredictable, and failure to notice in time by caretakers may lead to life-threatening outcomes. Scalp electroencephalography (EEG) is a widely used, non-invasive technique for seizure monitoring and detection, which directly measures neuronal electrical activities in high temporal resolution. However, the complex and chaotic underlying dynamics of human EEG systems is relatively difficult to be captured using conventional signal processing methods (i.e., Fourier transform or wavelet transform) due to the non-linearity and non-stationarity of EEG signals. One of the major challenges of seizure detection/prediction is to find appropriate representations of EEG recordings such that epileptic patterns are most differentiable from non-epileptic patterns. Chaos theory has recently been employed for nonlinear time series analysis because it enables novel feature extraction methods which are suitable for characterizing the chaotic features of EEG signals [2]. To this end, quantitative metrics extracted from recurrence plots [3] have been applied to detect the transition from normal states to seizure onsets in epileptic brains [4]–[7].

The synchronization processes (the simultaneous activity of multiple units) have long been discussed in order to understand the mechanism of human epileptic brains [8]. Complex system theory, which models human brain as a complex system comprised of interactive units (e.g., EEG channels), indicates that the underlying dynamics of epilepsy can be assessed through synchronization phenomena [9]–[11]. In recent decades, the emergence of complex network theory has inspired a number of studies to utilize network analysis for characterizing epileptic brains based on EEG [12]–[15]. Although the global and local spatial synchronization/interrelationship patterns are investigated in existing studies by converting multivariate EEG signals to network representation, only few studies have explored the temporal synchronization patterns in epileptic brains [16], [17]. However, evidences were found that the increased temporal inter-dependencies also help capture the collective dynamics of firing neurons in epileptic EEG system from a novel perspective and therefore worthy of further study [18].

In the present study, we proposed a multivariate seizure detection approach that represents the EEG signals using based on the concept of recurrence network (RN) [19], and further integrate it with spectral graph theory [20] to characterize the spatio-temoporal synchronization in large-scale EEG recordings. The objective of our study is two-fold: (1) to extend RN to a multivariate space that enables simultaneous integration of spatial and temporal recurrence patterns; and (2) to explore the applicability of spectral graph theoretic feature (i.e., eigenvalue) associated with RN for detecting seizure onsets efficiently. With validation on a benchmark database [21], we also discussed the insights of synchronization phenomena during seizure onsets in

Manuscript received September 28, 2017; revised March 23, 2018 and May 29, 2018; accepted June 15, 2018. Date of publication June 27, 2018; date of current version February 18, 2019. This work was supported by the National Science Foundation (Award No: CMMI 1538059) and Northeastern Faculty Startup Fund. *(Corresponding author: Chun-An Chou.)*

The authors are with the Department of Mechanical and Industrial Engineering, Northeastern University, Boston, MA 02115 USA (e-mail: fan.mi@husky.neu.edu; ch.chou@northeastern.edu).

This paper has supplementary downloadable material available at http://ieeexplore.ieee.org, provided by the author. The file is a PDF and the size is 1 MB.

Digital Object Identifier 10.1109/TBME.2018.2850959

order to enhance our understanding of the underlying epileptic mechanisms.

The reminder of this paper is organized as follows. Section II briefly reviews relevant studies on the seizure detection, particularly focuses on those who investigated the suitability of network analysis over temporal interdependency relationship. Section III illustrates the methodological framework of the present work. Section IV presents the empirical results based on a benchmark scalp EEG database of epileptic patients. Section V discusses results of our proposed model comparing to alternative models and previous studies. Section VI summarizes the concluding remarks as well as future directions of our study.

II. Related Work

To date, numerous automatic algorithms have been developed for seizure detection or prediction based on signal processing techniques. Many public databases are now available for testing new algorithms, such as CHB-MIT scalp EEG dataset published by PhysioNet [22]. In particular, the nonlinearity of EEG signals need to be addressed with nonlinear methods, including decomposition methods which are free from linearity assumption of signals (i.e. wavelet transform [23] or empirical mode decomposition [24], [25]) and nonlinear feature extraction (i.e. entropic features [26] or recurrence quantification analysis (RQA) [27], [28]). RQA was developed based on recurrence plot (RP) [3], which visualizes the recurrence patterns of the reconstructed state space trajectory, for characterizing the chaotic behaviors of complex systems. In our previous studies, we found RQA measures effective for capturing transient states in various scenarios using EEG signals [29], [30]. Nevertheless, applying the conventional RP to multivariate time series is more challenging due to the signal complexity in nonlinear, high-dimensional space. To reconstruct chaotic dynamics from an univariate dynamical system, for instance, an integer-valued estimate for the dimensions of a strange attractor is typically obtained through a false-nearest-neighbors approach [31]. In a multivariate dynamical system, however, the optimal dimensionality may be fractal [32] or may vary for different observation channels (e.g., as suggested by [33], [34]). Accordingly, a multivariate reconstruction approach was proposed, which demonstrated a better recovery of the chaotic dynamics [33], [34].

To bridge between multivariate EEG time series and complex network theory, some novel approaches were proposed by varying the definition of nodes and edges in network models. [16], [17] represented EEG signals using a weighted visibility graph (VG), where each node corresponds to one time point, and the inter-dependency relationships among time points are mapped into a weighted network. The topological features (i.e. average weighted degree) of VG were then computed to distinguish epileptic from non-epileptic EEG signals using machine learning algorithms. Similarly, RN [19] represents the temporal dependency relationship using network models, where each node corresponds to the system's state that can be jointly defined based on the information from the past, present and future states. It was reported that epileptic EEG signals have denser connections and higher cluttering coefficient compared to normal states in these network models [12]. In addition, the structural complexity and inter-dependency was found to be increased in epileptic EEG signals [14], [35]. Comparing to conventional RQA measures, RN-based network measures may be more suitable for seizure detection as suggested by previous studies [15]. In overall, these findings indicate the potential of RN-based network analysis approach for seizure detection, which has not been explicitly revealed yet.

III. Methodology

In this section, we present a framework for characterizing the temporal dynamics in EEG signals based on chaos theory and spectral graph theory. Figure 1 illustrates our methodological framework. Firstly, EEG signals are segmented via sliding time window (of one second); secondly, each segment of multivariate EEG signals is mapped into an $n-$dimensional state space through representing each state of the EEG system by a state vector. The state space trajectory is then reconstructed to describe how the system evolves over time. Thirdly, the recurrence pattern is characterized by a RP that represents the neighborhood relationship among system states in the reconstructed space. RN is then constructed by re-interpreting each RP matrix as the adjacency matrix. Subsequently, spectral graph theory is introduced for extracting global topological features (Fielder number) from RN. Finally, a statistical control chart is applied on the extracted features for detecting seizure onsets by monitoring abnormal changes in network synchronization. In addition, the conventional RQA measures are computed in order to compare with the spectral graph theoretic features.

A. Graphical Representation of Multivariate EEG Signals

According to Takens' embedding Theorem [36], the structure of underlying dynamics for chaotic systems (i.e., multivariate EEG signals) is reconstructed using a time-delayed embedding method. In the state space, the ith state of the system is denoted by $\mathbf{x}_i$ with m units, that is, $\mathbf{x}_i = (v_{1+(i-1)\tau}, \ldots, v_{m+(i-1)\tau}), i \in 1, \ldots, T$ in a sliding window of T states, where v_t is observation collected at time t, and m and τ are the parameters of embedding dimension and time delay, respectively. Then, RP is computed by the following formula to represent the recurrence pattern (i.e., the system's states at different times are close to each other in the state space) of multivariate EEG signals:

$$\mathbf{R}_{i,j} = \Theta(\varepsilon - \|\mathbf{x}_i - \mathbf{x}_j\|),\ \mathbf{x}_i, \mathbf{x}_j \in \mathbb{R}^m,\ i, j = 1, ..., T, \quad (1)$$

where $\Theta(\cdot)$ is the Heaviside function and ε is a threshold to determine the neighborhood relationship. $\|\cdot\|$ quantifies the distance between any two points on the state space trajectory. In the present study, we choose Euclidean distance to measure the distance between system states and the corresponding distance matrix is denoted as $\mathbf{R}^*_{i,j}$. We herein propose two models for representing the recurrence patterns of multivariate epileptic EEG signals.

Model I. In Model I, we present a multivariate generalization of RP extended from univariate time series, as suggested by [37], to represent the n-dimensional system. We do not consider a time-delay embedding ($m = 1$ and $\tau = 1$) in this Model. The ith state of the system is now represented by a column vector $\mathbf{x}_i$, consisting of the observation in n channels.

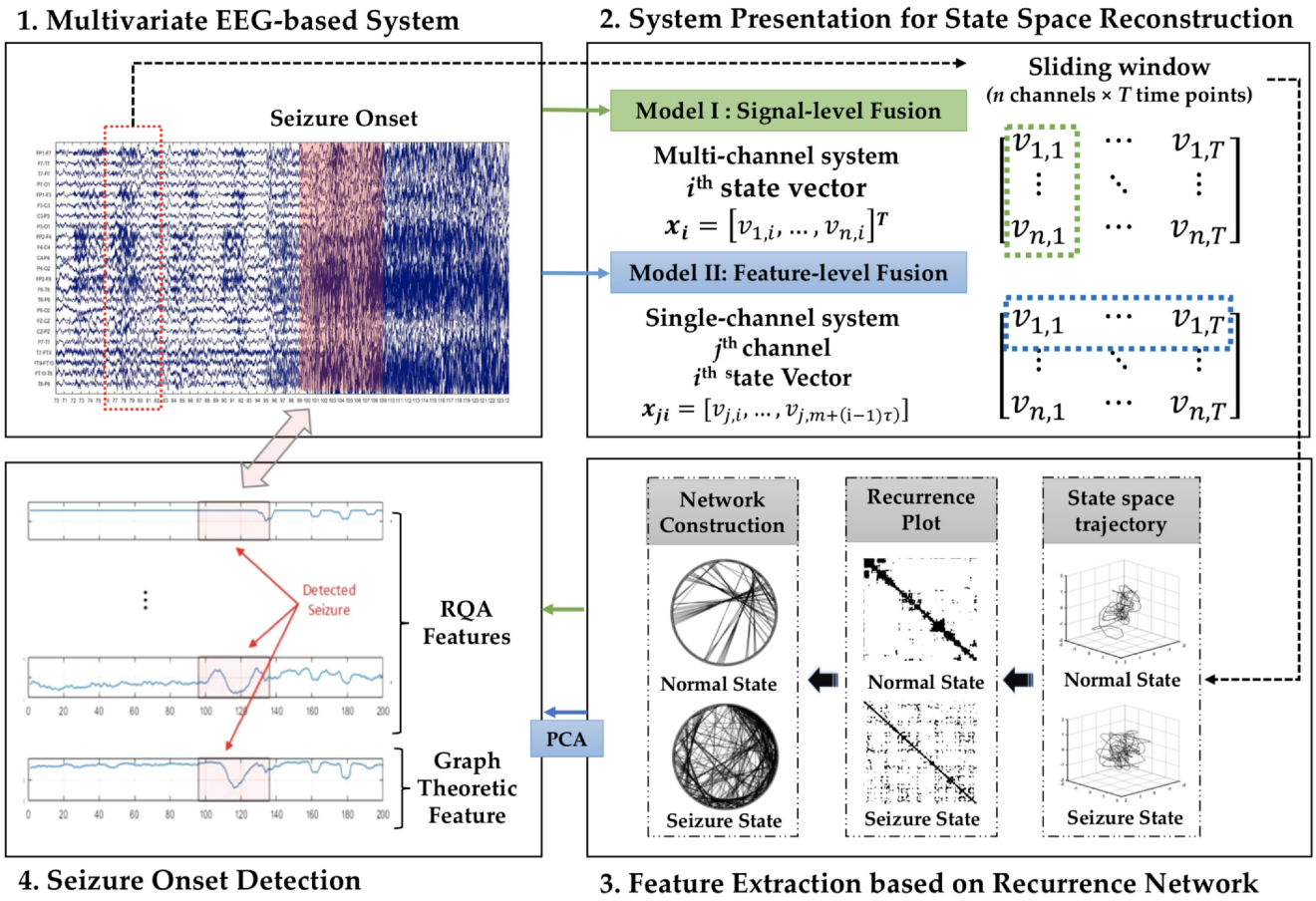

Fig. 1. An illustration of the proposed analytical framework. (1) The multivariate EEG signals are segmented within sliding windows (1 s). (2) The state space reconstruction is conducted in two ways: in Model I, the system state at time i is represented by a n-dimensional vector x_i; in Model II, the system state at time i is represented by a m-dimensional time-delayed vector. (3) The temporal structure of the system dynamics (neighborhood relationship among the points on state space trajectory) is represented by RP and corresponding RN. RQA features and graph theoretic features (λ_2) are extracted, respectively, from RP and RN. (4) A statistical control chart is applied to time series of features for detecting seizure onsets. As the sliding window proceeds, the system state is monitored by tracking these feature values for a real-time detection. Note that in Model II, the RQA features and graph theoretic feature extracted from individual channels are fused by PCA.

Model II. In Model II, EEG signals collected from each channel are individually processed using the time-delayed embedding method for reconstructing state space trajectory [36]. Specifically, we take $m = 3$ and $\tau = 5$, as estimated by false nearest neighbor and mutual information method.

Next, a selection of RQA features and graph theoretic features are extracted from the RP constructed in Model I and Model II. The details of extracting RQA features from RP are included in supplementary materials. The adjacency matrix of RN, $\mathbf{A}_{i,j}(\varepsilon)$, is then converted as follows:

$$\mathbf{A}_{i,j}(\varepsilon) = \mathbf{R}_{i,j}(\varepsilon) - \mathbf{I}(T), \tag{2}$$

where $\mathbf{R}_{i,j}(\varepsilon)$ is RP with threshold $= (\varepsilon)$ and $\mathbf{I}(T)$ is $T-$dimensional identity matrix for removing the self-loops [38]. Note that in the present study, each node in RN corresponds to a column vector which describes the state of the multivariate EEG system at a certain time point. Thus, RN is used in our study to present the state space synchronization considering the spatio-temporal information of multivariate time series.

B. Spectral Graph Theoretic Feature Extraction

Spectral graph theory [20] is the mathematical study that bridges between linear algebra and graph theory by applying eigen-decomposition to matrices representation of graphs (e.g. adjacency or Laplacian matrices) in order to reveal their topological properties. The Laplacian matrix of RN is defined as $\mathbf{L} = \mathbf{D} - \mathbf{A}_{i,j}(\varepsilon)$, where $\mathbf{D} = d_{ij}$ is the diagonal matrix and d_{ii} is the ith node's degree. The eigenvalues and eigenvectors are obtained by applying eigen-decomposition to Laplacian matrix L of RN, and we are particularly interested in the second smallest eigenvalue λ_2 (also referred to as Fiedler number [39]), a metric for algebraic connectivity that help us characterize the synchronizability of RN. In general, a network with a higher value of λ_2 is more synchronized, namely, its nodes are more likely to be driven by common dynamics, and vice versa. An illustrative example is presented in Figure 2. Given a sliding window of nine time points $\{T_1, \ldots, T_9\}$, the complete graph (i.e., all nodes are connected with each other) in left panel yields $\lambda_2 = 9$ and suggests a strong synchronizability, while the graph

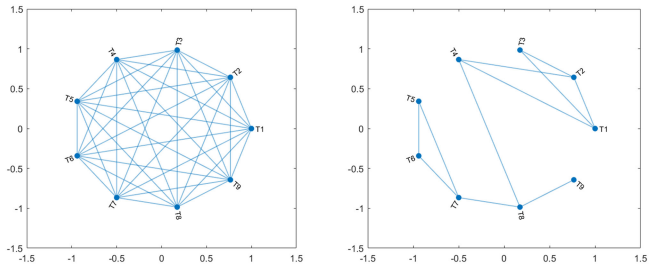

Fig. 2. An example to illustrate how Fiedler number quantifies the synchronizability of a graph. In our study, the nodes in network represent different states of the dynamical system over time, and the edges represent the temporal dependencies among the states. A strong temporal synchronization of the system is characterized by a high value of λ_2 (left panel) during the present time period, whereas a weak temporal synchronization of the system is characterized by a low value of λ_2 (right panel).

with partial connections in right panel yields $\lambda_2 = 0.2229$ and suggests a weak synchronizability.

To investigate the impact of thresholding RN, we apply eigen-decomposition to both unthresholded RN (the distance matrices $\mathbf{R}^*_{i,j}$) and thresholded RN (the binary matrices $\mathbf{R}_{i,j}(\varepsilon)$), and denote the corresponding spectral graph theoretic features λ_2^d and λ_2^b respectively. We intend to examine whether or not richer information is preserved in unthresholded RN than thresholded RN by comparing λ_2^d to λ_2^b. Since extracting λ_2^d does not require the parameter tuning for threshold ε (in Equation (1)) it yields the advantage of lower computational cost as well as reduced model complexity.

C. Seizure Detection Using Control Chart

For each type of feature, the extracted feature values (e.g., λ_2) are concatenated in a temporal sequence to represent the original time series EEG signals. As we have a short time window, some sharp fluctuations are expected for certain features and thus a five-point moving average filter is applied for smoothing the new time series. In Model II, we first apply principal component analysis (PCA) to the 23-dimensional vector of each feature and obtain the top 10 principal components in order to account for over 80% variation on average. Then, the multivariate Hotelling T^2 control chart [40] is applied to the dimensionality-reduced feature vector (dimensionality = 10) with 95% CI for seizure detection. The Hotelling T^2 is a multivariate distance metric which takes the multivariate covariances into consideration assuming the multivariate normal distribution, proposed as a generalization of Student's-t statistic. As suggested in [41], PCA is applied prior to the control chart to lessen the impact of autocorrelation in time series on the performance of Hotelling T^2. The mathematical definition is as follows:

$$T^2 = c(\mathbf{X} - \mathbf{m}')\mathbf{S}^{-1}(\mathbf{X} - \mathbf{m}), \tag{3}$$

where $\mathbf{X}$ is the multivariate sample matrix, $\mathbf{m}'$ is the mean, $\mathbf{S}$ is the covariance matrix, and c is a constant accounting for the sample size. In Model I, a statistical control chart of mean is used for seizure onset detection. The upper control limit (UCL) and lower control limit (LCL) are defined as follows:

$$UCL = \hat{\mu} + k \times \hat{\sigma}, \tag{4}$$

$$LCL = \hat{\mu} - k \times \hat{\sigma}, \tag{5}$$

where $\hat{\mu}$ and $\hat{\sigma}$ are the estimates of mean and standard deviation, respectively, and k is the parameter that determines control limits. We therefore select $k = 3$, as the 3σ limit (average plus and minus 3 times standard deviation) is a common criteria in statistical control chart that ensures 99.73% of total observations are within control limits (assuming the normal distribution). The alarm will be triggered when 2 of 3 points fall below LCL or above UCL (same side). In addition, the first 180 windows (3 minutes) located at the beginning of each session are used for estimating $\hat{\mu}$ and $\hat{\sigma}$ for the corresponding session.

D. Performance Evaluation and Model Validation

To evaluate the effectiveness and robustness, our proposed method is tested on three types of data: (1) the original CHB-MIT EEG signals; (2) the band-decomposed EEG signals and (3) the EEG signals with white noise and surrogate noise at different levels. Various performance metrics in seizure detection tasks include *sensitivity*, *false alarm rate (FAR)*, and *latency*. Sensitivity is defined as the proportion of detected seizure periods, which means the alarm has been triggered in the duration of seizure onset zone. FAR is defined as the ratio of non-epileptic alert events to the true negative events. Latency is defined as the time lag (in second) between the start of seizure onset and the earliest alert.

IV. Experimental Results

A. Dataset Description and Preprocessing

CHB-MIT scalp EEG dataset [21], [22] is used for testing our proposed method. CHB-MIT is a benchmark public database that consists of EEG recordings from 23 epileptic patients at Boston Children's Hospital (5 males of age from 3 to 22; 17 females of age from 1.5 to 19. For a brief summary see Table I). The EEG signals were recorded during many days using the International 10–20 system of 23 electrodes with a sampling rate of 256 Hz. 182 epileptic epochs were marked by domain experts in a subset of sessions ($N = 129$) of the CHB-MIT dataset. Note that we only employed the sessions with seizure onset epochs. After baseline removal and normalization, the EEG signals were re-referenced to average and a band-pass filter of $1 \sim 50$ Hz was applied to reduce noise in the signals. These pre-processing steps were performed using functions in EEGLAB toolbox [42]. Then, a non-overlapping sliding window of 1 second length was applied to each session of EEG recordings to split the signals into segments.

B. Overall Performances

Table II shows a summary of overall performance metrics averaged across all subjects. Performances for each individual subject are provided in the supplementary materials. We found TT feature yielded the best average sensitivity of 98.48%. In

TABLE I
SUMMARY OF PATIENT STATISTICS

ID	Gender	Age	No. of seizures	No. of sessions
1	F	11	7	7
2	M	11	3	3
3	F	14	7	7
4	M	22	4	3
5	F	7	5	5
6	F	1.5	10	7
7	F	14.5	3	3
8	M	3.5	5	5
9	F	10	4	3
10	M	3	7	7
11	F	12	3	3
12	F	2	40	13
13	F	3	12	8
14	F	9	8	7
15	M	16	20	14
16	F	7	10	6
17	F	12	3	3
18	F	18	6	6
19	F	19	3	3
20	F	6	8	6
21	F	13	4	4
22	F	9	3	3
23	F	6	7	3
Sum			182	129

TABLE II
PERFORMANCES SUMMARY

Approach	Sensitivity	FAR	Latency*
Model I			
LMAX	55.49%	15.70%	6.45
TND	88.46%	17.10%	10.70
LAM	56.58%	14.43%	**6.03**
TT	**98.48%**	21.40%	8.59
λ_2^b	54.81%	**8.61%**	6.54
λ_2^d	97.46%	15.94%	7.27
Model II			
LMAX	79.12%	14.98%	6.11
TND	85.16%	**13.63%**	7.57
LAM	81.32%	15.67%	8.77
TT	76.92%	14.70%	10.96
λ_2^b	81.87%	20.07%	**4.78**
λ_2^d	**90.11%**	14.49%	5.47
Other Studies			
Shoeb [34]	96.00%	5/hr **	4.60
Ahammad et al. [5]	98.5%	14.4%	1.76
Thodoro et al. [41]	85%	0.8/hr **	Not Reported
Samiee et al. [33]	70.19%	2.26%	Not Reported
Samiee et al. [32]	70.4%	0.35/hr **	Not Reported
Zabihi et al. [49]	88.27%	6.79%	Not Reported
Bhattacharyya and Pachori [6]	97.91%	0.43%	Not Reported
Khanmohammadi and Chou [22]	96.00%	0.12/hr**	4.21

The best results obtained are highlighted in bold.
* Time unit is second.
** In these studies, the false alarm rate is reported as the number of false alarms per hour.
*** Not reported.

addition, the λ_2^d feature has a comparable level of sensitivity (97.46%). The λ_2^b feature yields the lowest FAR (8.61%), which indicates it is more robust to the changes in signals caused by non-seizure events. The shortest latency (6.03 seconds) is observed in LAM feature, and most features can detect seizure onsets within 8 seconds.

Low computational cost is a worth-mentioned advantage of our method to show high capacity for real-time applications. The computational cost of a detection algorithm is defined as the average processing time required for each sliding window (a segment that contains all channels), which includes feature extraction and model training processes. Specifically, the time delay of an alert increases when the computational cost per window is longer than the window length. In Model I, there is no cost for parameter tuning in the embedding dimensions using a multivariate representation of RP. A significant improvement in computational time (0.06 second per window) is achieved because all channels were processed simultaneously. In short, the multi-channel signals can be converted (and fused) to RPs more efficiently, which makes it more suitable for a real-time scenario.

C. Comparison Between Multivariate and Univariate RP Construction

As shown in Table II , LMAX, LAM and λ_2^b features have better sensitivity in Model II, while TND, TT and λ_2^d features have better sensitivity in Model I. Namely, processing the information from each EEG channel individually does not improve detection sensitivity for TND, TT and λ_2^d features when using multi-channel control chart. On the other hand, the shortest latency (4.78 sec) is achieved in Model II. However, since the computational cost of Model II is also increased to 1.6–2 seconds per window, which is longer than the window length, it is not feasible for real-time detection scenarios.

D. Comparison Between RQA Measures and Graph Theoretic Measures

Figure 3 displays the temporal behaviors based on RQA measures and graph theoretic measure. The graph theoretic features yield more stable performances in seizure detection, while RQA measures exhibit relatively large variations. The possible causes of these variations may be (1) the noise in EEG signals, and/or (2) RQA measures rely on a fine parameter tuning, especially the threshold selection. In contrast, the λ_2^d feature is independent of threshold selection. The experimental results of our study in Model I also suggest that λ_2^d feature is more sensitive than some RQA features (e.g., TND and LAM features in Figure 3) for detecting the transient point, which may indicate a change from normal state to epileptic state. In addition, a two-sample Student's Test with 95% confidence level shows that λ_2^d feature value is significantly higher in seizure onset periods than normal states in 105 out of 129 sessions. All the above observations lend support to the hypothesis that the spectral graph theoretic features have better potential in detecting seizure onsets

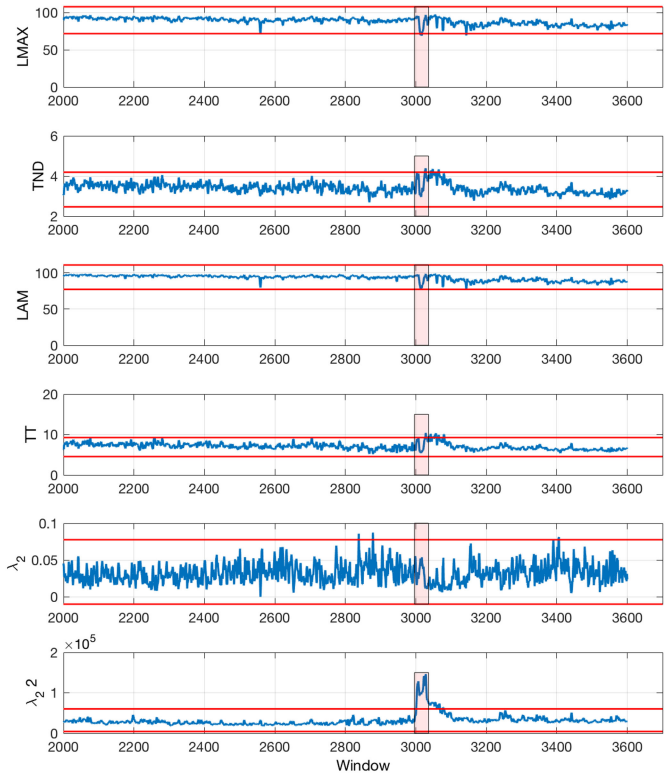

Fig. 3. The control chart is applied to monitor dynamical changes of RQA and graph theoretic features. The highlighted segments (in red shadows) are the seizure onset periods. This is an illustrative example from session 3 of Subject 1.

comparing to conventional RQA measures. The interpretation of this observation will be further described in Section V.

E. Testing for Robustness for Model I

The robustness of Model I is tested by adding white noise and surrogate noise with signal-to-noise ratio (SNR) $= \{0.1, 0.3, 0.5, 0.7\}$. As shown in Table III, both the white noise and surrogate noise have obvious negative impact on our model performances. TND feature is shown to be most robust and sensitive comparing to others in majority tests. λ_2^b feature yields the lowest sensitivity, which suggests a significant influence from noise. An interesting observation is that the influence on the performance does not have a linear correlation with the SNR. Adversely, our experiment shows that some features may even be more sensitive with a stronger surrogate noise; meanwhile, all levels of the white noise have a similar impact.

F. Band Decomposition

In order to investigate the effect of band-pass decomposition, we applied our proposed method independently to band-pass filtered signals to find if there are any frequency bands particularly useful for seizure detection, including (1) Alpha waves (8−12 Hz) (2) beta waves (12−40 Hz) (3) Theta waves (1−4 Hz) (4) Delta waves (4−8 Hz). Next, we applied the procedure described in Model I to each band-passed signals. Table IV shows the performance metrics after band decomposition. In general, the decomposition has best performances using Beta band (in sensitivity) and Alpha band (in FAR and latency), and the overall FAR and latency is improved as well. Moreover, the λ_2^d feature yields best sensitivity in all bands. However, comparing to previous studies using spectral analysis, decomposing EEG signals into different brain waves does not improve the performances of our method significantly, although some waves are shown to be more informative than others in detecting seizure onsets events.

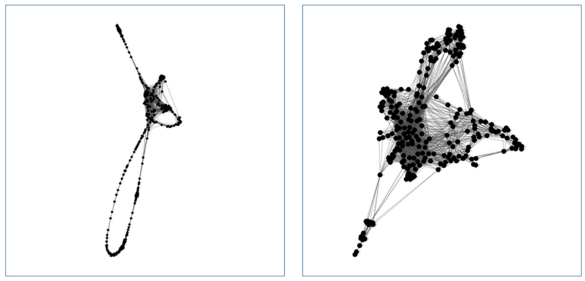

Fig. 4. A visualization of temporal synchronization patterns constructed from seizure onsets (left panel) and normal state signals (right panel), respectively. Both networks are identical in connectivity density, but the normal state has a spread-out distribution of the recurrence network, indicating the states per second are less synchronized during normal period than seizure onset period.

V. Discussions

We have shown that the algebraic connectivity of recurrence networks is significantly increased ($\alpha = 0.05$) in 81% of total sessions during seizure onset periods. This finding provides some interesting insights that may help understand the epileptic processes. In consistent to [16], our study has evidenced the seizure onset can also be characterized by a dramatic increase in synchronization of short time (1 second) temporal proximity between state vectors. This finding provides a novel perspective of utilizing the temporal information in neurological time courses to build connectivity patterns for studying dynamical transitions between order and chaos. The nonlinear dynamics of normal/epileptic brains driven by chaotic attractor might be revealed by the topological characteristics of such graphs. In Figure 4, the network representing the synchronization patterns over time are visualized using sample data from Subject 1.

Comparing to the typical framework of RQA-based seizure detection using multi-channel EEG data, our method yields several advantages. Firstly, our method requires neither channel/feature selection process nor band-decomposition. This feature has greatly simplified the procedure and saves computational cost, which makes our method more suitable to be embedded in real-time detection setting for clinical practices (i.e., it performs well even on portable devices of limited computation resources). Moreover, the sensitivity and latency metrics have shown that λ_2^d is more sensitive to the transition from normal states to epileptic states than the selected RQA measures in all tested models (multivariate/univariate, original/band-passed signals) in such a EEG-based chaotic system. Finally, as previous studies formulated the seizure detection

TABLE III
PERFORMANCE METRICS OF MODEL I WITH SIMULATED NOISE

	White Noise (SNR = 0.1)			White Noise (SNR = 0.3)			White Noise (SNR = 0.5)			White Noise (SNR = 0.7)		
	Sensitivity	FAR	Latency	Sensitivity	FAR	Latency	Sensitivity	FAR	Latency	Sensitivity	FAR	Latency
LMAX	67.03%	8.53%	22.20	70.33%	13.55%	19.70	68.13%	11.56%	20.79	69.02%	12.48%	18.16
TND	72.53%	5.25%	22.96	73.08%	10.94%	22.99	73.08%	12.71%	19.69	71.74%	13.80%	16.46
LAM	69.78%	9.86%	22.28	68.13%	13.77%	18.82	68.68%	14.67%	20.39	69.02%	15.38%	18.79
TT	70.33%	6.74%	22.22	69.78%	11.72%	18.08	68.68%	12.11%	17.78	68.48%	12.88%	16.70
λ_2^b	59.89%	2.41%	33.48	64.84%	3.94%	27.71	72.53%	5.20%	24.83	71.74%	6.13%	23.40
λ_2^d	73.08%	11.27%	20.04	68.68%	15.27%	17.01	70.33%	16.25%	17.60	70.65%	16.88%	18.03
	Surrogate Noise (SNR = 0.1)			**Surrogate Noise (SNR = 0.3)**			**Surrogate Noise (SNR = 0.5)**			**Surrogate Noise (SNR = 0.7)**		
	Sensitivity	FAR	Latency	Sensitivity	FAR	Latency	Sensitivity	FAR	Latency	Sensitivity	FAR	Latency
LMAX	60.53%	12.07%	20.06	63.74%	10.87%	19.78	64.84%	9.60%	27.83	64.48%	8.56%	26.69
TND	70.00%	14.73%	25.17	70.33%	12.98%	25.63	69.23%	11.01%	23.85	71.58%	9.40%	22.25
LAM	61.05%	12.86%	19.91	65.93%	11.79%	23.12	68.13%	10.35%	24.33	68.31%	9.23%	23.77
TT	64.21%	14.70%	25.81	65.38%	13.82%	22.91	70.88%	12.33%	21.24	73.22%	11.01%	23.31
λ_2^b	63.16%	7.49%	29.26	67.03%	6.67%	28.06	68.68%	5.89%	23.11	67.21%	5.43%	22.96
λ_2^d	68.95%	18.10%	17.68	71.98%	18.40%	18.26	70.33%	17.72%	18.10	69.40%	16.74%	19.03

TABLE IV
PERFORMANCE METRICS AFTER BAND DECOMPOSITION OF SIGNAL-LEVEL FUSED DATA

Band	Alpha			Beta			Theta			Delta		
Metrics	Sensitivity	FAR	Latency	Sensitivity	FAR	Latency	Sensitivity	FAR	Latency	Sensitivity	FAR	Latency
LMAX	79.12%	9.32%	12.88	81.32%	22.88%	**6.65**	67.03%	8.66%	15.25	51.10%	7.27%	13.69
TND	65.38%	**6.73%**	14.54	68.68%	**13.24%**	11.26	**79.12%**	**8.19%**	9.75	76.37%	**8.44%**	10.79
LAM	79.12%	12.51%	10.32	80.77%	23.94%	7.91	62.64%	9.42%	14.65	47.80%	8.60%	13.90
TT	63.19%	8.14%	11.98	70.88%	14.26%	12.91	74.18%	9.31%	8.74	74.18%	10.52%	**6.75**
λ_2^b	57.69%	8.88%	17.66	62.09%	14.34%	12.73	60.44%	8.72%	15.32	72.53%	8.56%	8.50
λ_2^d	**81.32%**	19.53%	**4.50**	**82.42%**	25.08%	7.38	**79.12%**	17.00%	**4.38**	**80.22%**	18.94%	8.94

The best results obtained are highlighted in bold.

problem as a classification task [21], [44], [48], our method takes advantage of the computational efficiency in statistical control chart for real-time detection, in which no intensive model training process is required in our proposed method. On the other hand, since the projection from time series to the state space involves no time-delay embedding, a significant decrease in computational cost should be expected accordingly. Unlike in previous literature [49], a visual inspection is not required for selecting time-delay embedding parameters in our method and therefore the complexity of model can be significantly reduced with the number or tuning parameters.

Although our study has achieved its goals in theoretical and practical perspectives, there are still some limitations of our method. Firstly, the metric $\lambda_2^b = 0$ for a disconnected graph and therefore it failed to provide further topological information in such cases. Accordingly, the threshold value for binarizing the distance matrix should be selected with caution. Secondly, our approach was tested on a fixed time window (1 second) with 50% overlap, which means each time window moves 500 ms forward. Given that the rapid transition from normal to epileptic states may even happen in less than 500 ms, it is worthy of consideration that the change in temporal synchronization pattern could slightly varies when analyzed with multiple time scales. Finally, the sensitivity for short seizure periods, as well as the robustness for long periods of our approach need to be improved. For example, the λ_2^d feature shows a low sensitivity on Subject 6 and Subject 12, whose seizure periods are sometimes short (10–20 seconds). It may imply that the length of seizure onsets will limit the performances of our proposed method when the seizure onsets ended before the change of EEG states could be detected. However, this hypothesis can not explain few cases, e.g., Subject 15 and Subject 16. Since the CHB-MIT database only provides limited patient information, the impact of other factors such as seizure type remains to be evaluated in the future on other datasets.

VI. CONCLUSIONS

In this study, we presented a new approach to detect seizure onset events by characterizing the temporal synchronization pattern of multivariate EEG signals, in which multi-channel EEG signals are fused at signal level. We presented the complex EEG-based epileptic brain system as a recurrence network and found that the graph theoretic features associated with it can characterize the synchronization structures of epileptic brain network. Our experimental results showed a high sensitivity of 98.48%; seizure onsets are detected successfully for most subjects (except for Subject 12) in the test dataset. More importantly, our approach is potentially useful for patient-specific (or personalized) diagnosis and treatments without information from other subjects to be pre-trained. In the future work, we may consider adaptive threshold parameters applied to sliding

windows and sensitivity analysis of different window lengths, which allows us to explore the time-varying dynamics of epileptic brain networks from multiple temporal scales.

REFERENCES

[1] Epilepsy Foundation, "A revised definition of epilepsy," Landover, MD, USA, Apr. 2014. [Online]. Available: http://www.epilepsy.com/article/2014/4/revised-definition-epilepsy

[2] C. Stam *et al.*, "Dynamics of the human alpha rhythm: Evidence for non-linearity?" *Clin. Neurophysiol.*, vol. 110, no. 10, pp. 1801–1813, 1999.

[3] J.-P. Eckmann *et al.*, "Recurrence plots of dynamical systems," *Europhys. Lett.*, vol. 4, no. 9, pp. 973–977, 1987.

[4] N. Thomasson *et al.*, "Recurrence quantification in epileptic EEGs," *Phys. Lett. A*, vol. 279, no. 1, pp. 94–101, 2001.

[5] U. R. Acharya *et al.*, "Application of recurrence quantification analysis for the automated identification of epileptic EEG signals," *Int. J. Neural Syst.*, vol. 21, no. 03, pp. 199–211, 2011.

[6] M. Niknazar *et al.*, "A new framework based on recurrence quantification analysis for epileptic seizure detection," *IEEE J. Biomed. Health Informat.*, vol. 17, no. 3, pp. 572–578, May 2013.

[7] L. Murali *et al.*, "An efficient adaptive filter architecture for improving the seizure detection in EEG signal," *Circuits, Syst., Signal Process.*, vol. 35, no. 8, pp. 2914–2931, 2016.

[8] K. Lehnertz *et al.*, "Synchronization phenomena in human epileptic brain networks," *J. Neurosci. Methods*, vol. 183, no. 1, pp. 42–48, 2009.

[9] R. Friedrich and C. Uhl, "Spatio-temporal analysis of human electroencephalograms: Petit-mal epilepsy," *Phys. D: Nonlinear Phenom.*, vol. 98, no. 1, pp. 171–182, 1996.

[10] M. Winterhalder *et al.*, "Spatio-temporal patient–individual assessment of synchronization changes for epileptic seizure prediction," *Clin. Neurophysiol.*, vol. 117, no. 11, pp. 2399–2413, 2006.

[11] P. Mirowski *et al.*, "Classification of patterns of EEG synchronization for seizure prediction," *Clini. Neurophysiol.*, vol. 120, no. 11, pp. 1927–1940, 2009.

[12] P. Lang *et al.*, "Recurrence network analysis of the synchronous EEG time series in normal and epileptic brains," *Cell Biochem. Biophys.*, vol. 66, no. 2, pp. 331–336, 2013.

[13] Z.-K. Gao *et al.*, "Recurrence networks from multivariate signals for uncovering dynamic transitions of horizontal oil-water stratified flows," *Europhys. Lett.*, vol. 103, no. 5, p. 50004, 2013.

[14] N. P. Subramaniyam and J. Hyttinen, "Characterization of dynamical systems under noise using recurrence networks: Application to simulated and EEG data," *Phys. Lett. A*, vol. 378, no. 46, pp. 3464–3474, 2014.

[15] E. J. Ngamga *et al.*, "Evaluation of selected recurrence measures in discriminating pre-ictal and inter-ictal periods from epileptic EEG data," *Phys. Lett. A*, vol. 380, no. 16, pp. 1419–1425, 2016.

[16] S. Supriya *et al.*, "Weighted visibility graph with complex network features in the detection of epilepsy," *IEEE Access*, vol. 4, pp. 6554–6566, 2016.

[17] S. Supriya *et al.*, "Automatic epilepsy detection from EEG introducing a new edge weight method in the complex network," *Electron. Lett.*, vol. 52, no. 17, pp. 1430–1432, 2016.

[18] S. Bialonski and K. Lehnertz, "Identifying phase synchronization clusters in spatially extended dynamical systems," *Phys. Rev. E*, vol. 74, no. 5, p. 051909, 2006.

[19] R. V. Donner *et al.*, "Recurrence networks—A novel paradigm for nonlinear time series analysis," *New J. Phys.*, vol. 12, no. 3, pp. 033025, 2010.

[20] F. R. Chung, *Spectral Graph Theory*, vol. 92. Philadelphia, PA, USA: American Mathematical Soc., 1997.

[21] A. H. Shoeb, "Application of machine learning to epileptic seizure onset detection and treatment," Ph.D. dissertation, Massachusetts Inst. Technol., Cambridge, MA, USA, 2009.

[22] A. L. Goldberger *et al.*, "Physiobank, physiotoolkit, and physionet," *Circulation*, vol. 101, no. 23, pp. e215–e220, 2000.

[23] A. Bhattacharyya and R. B. Pachori, "A multivariate approach for patient-specific EEG seizure detection using empirical wavelet transform," *IEEE Trans. Biomed. Eng.*, vol. 64, no. 9, pp. 2003–2015, Sep. 2017.

[24] R. B. Pachori and V. Bajaj, "Analysis of normal and epileptic seizure EEG signals using empirical mode decomposition," *Comput. Methods Programs Biomed.*, vol. 104, no. 3, pp. 373–381, 2011.

[25] D. Cho *et al.*, "EEG-based prediction of epileptic seizures using phase synchronization elicited from noise-assisted multivariate empirical mode decomposition," *IEEE Trans. Neural Syst. Rehabil. Eng.*, vol. 25, no. 8, pp. 1309–1318, Aug. 2017.

[26] J. Xiang *et al.*, "The detection of epileptic seizure signals based on fuzzy entropy," *J. Neurosci. Methods*, vol. 243, pp. 18–25, 2015.

[27] J. P. Zbilut and C. L. Webber, "Embeddings and delays as derived from quantification of recurrence plots," *Phys. Lett. A*, vol. 171, no. 3–4, pp. 199–203, 1992.

[28] N. Marwan *et al.*, "Recurrence-plot-based measures of complexity and their application to heart-rate-variability data," *Phys. Rev. E*, vol. 66, no. 2, p. 026702, 2002.

[29] M. Fan *et al.*, "Acute stress detection using recurrence quantification analysis of electroencephalogram (EEG) signals," in *Proc. Int. Conf. Brain Informat. Health.* Omaha, NE, USA: Springer, 2016, pp. 252–261.

[30] M. Fan and C.-A. Chou, "Recognizing affective state patterns using regularized learning with nonlinear dynamical features of EEG," in *Proc. Int. Conf. Biomed. Health Informat.*, 2018, pp. 137–140.

[31] H. D. Abarbanel and M. B. Kennel, "Local false nearest neighbors and dynamical dimensions from observed chaotic data," *Phys. Rev. E*, vol. 47, no. 5, pp. 3057–3068, 1993.

[32] A. Accardo *et al.*, "Use of the fractal dimension for the analysis of electroencephalographic time series," *Biol. Cybern.*, vol. 77, no. 5, pp. 339–350, 1997.

[33] I. Vlachos and D. Kugiumtzis, "State space reconstruction from multiple time series," in *Proc. Topics Chaotic Syst.: Select. Papers Chaos Int. Conf.*, 2009, pp. 378–387.

[34] I. Vlachos and D. Kugiumtzis, "Nonuniform state-space reconstruction and coupling detection," *Phys. Rev. E*, vol. 82, no. 1, p. 016207, 2010.

[35] N. P. Subramaniyam and J. Hyttinen, "Dynamics of intracranial electroencephalographic recordings from epilepsy patients using univariate and bivariate recurrence networks," *Phys. Rev. E*, vol. 91, no. 2, pp. 022927, 2015.

[36] F. Takens, "Detecting strange attractors in turbulence," in *Dynamical Systems and Turbulence*, D. Rand and L.-S. Young, Eds. Berlin, Germany: Springer, 1981, pp. 366–381.

[37] C. L. Webber Jr and J. P. Zbilut, "Recurrence quantification analysis of nonlinear dynamical systems," *Tuts. Contemp. Nonlinear Methods Behav. Sci.*, pp. 26–94, 2005.

[38] R. V. Donner *et al.*, "Complex network analysis of recurrences," in *Recurrence Quantification Anal.*, C. L. Webber and N. Marwan, Eds. Berlin, Germany: Springer, 2015, pp. 101–163.

[39] M. Fiedler, "Algebraic connectivity of graphs," *Czechoslovak Math. J.*, vol. 23, no. 2, pp. 298–305, 1973.

[40] H. Hotelling, "Multivariate quality control," *in Techniques of Statistical Analysis*, C. Eisenhart, M. W. Hastay, and W. A. Wallis, Eds. New York, NY, USA: McGraw Hill, 1947, pp. 111–184.

[41] E. Vanhatalo and M. Kulahci, "Impact of autocorrelation on principal components and their use in statistical process control," *Quality Rel. Eng. Int.*, vol. 32, no. 4, pp. 1483–1500, 2016.

[42] A. Delorme and S. Makeig, "EEGLAB: An open source toolbox for analysis of single-trial EEG dynamics including independent component analysis," *J. Neurosci. Methods*, vol. 134, no. 1, pp. 9–21, 2004.

[43] N. Ahammad *et al.*, "Detection of epileptic seizure event and onset using EEG," *BioMed. Res. Int.*, vol. 2014, 2014.

[44] P. Thodoroff *et al.*, "Learning robust features using deep learning for automatic seizure detection," in *Proc. Mach. Learn. Healthcare Conf.*, 2016, pp. 178–190.

[45] K. Samiee *et al.*, "Long-term epileptic EEG classification via 2-D mapping and textural features," *Expert Syst. Appl.*, vol. 42, no. 20, pp. 7175–7185, 2015.

[46] K. Samiee *et al.*, "Epileptic seizure detection in long-term eeg records using sparse rational decomposition and local Gabor binary patterns feature extraction," *Knowl.-Based Syst.*, vol. 118, pp. 228–240, 2017.

[47] M. Zabihi *et al.*, "Analysis of high-dimensional phase space via poincaré section for patient-specific seizure detection," *IEEE Trans. Neural Syst. Rehabil. Eng.*, vol. 24, no. 3, pp. 386–398, Mar. 2016.

[48] S. Khanmohammadi and C.-A. Chou, "Adaptive seizure onset detection framework using a hybrid PCA-CSP approach," *IEEE J. Biomed. Health Informat.*, vol. 22, no. 1, pp. 154–160, Jan. 2018.

[49] N. Marwan, "How to avoid potential pitfalls in recurrence plot based data analysis," *Int. J. Bifurcation Chaos*, vol. 21, no. 4, pp. 1003–1017, 2011.